BJA

British Journal of Anaesthesia, 130 (3): 331–342 (2023)

doi: 10.1016/j.bja.2022.10.040
Advance Access Publication Date: 5 January 2023
Pain

Phenotype- and species-specific skin proteomic signatures for incision-induced pain in humans and mice

Daniel Segelcke[1,†], Max van der Burgt[1,†], Christin Kappert[2], Daniela Schmidt Garcia[2], Julia R. Sondermann[3], Stephan Bigalke[1,4], Bruno Pradier[1], David Gomez-Varela[3], Peter K. Zahn[4], Manuela Schmidt[3,*,‡] and Esther M. Pogatzki-Zahn[1,*,‡]

[1]Department of Anaesthesiology, Intensive Care and Pain Medicine, University Hospital Muenster, Muenster, Germany, [2]Max Planck Institute for Multidisciplinary Sciences, City Campus, Goettingen, Germany, [3]Division of Pharmacology and Toxicology, Department of Pharmaceutical Sciences, University of Vienna, Vienna, Austria and [4]Clinic for Anaesthesiology, Intensive and Pain Medicine, Ruhr-University Bochum, BG-University Hospital Bergmannsheil gGmbH, Bochum, Germany

*Corresponding authors. E-mails: manuela_schmidt@univie.ac.at, pogatzki@anit.uni-muenster.de
†These authors contributed equally.
‡These senior authors contributed equally.

Abstract

Background: Acute pain after surgery is common and often leads to chronic post-surgical pain, but neither treatment nor prevention is currently sufficient. We hypothesised that specific protein networks (protein-protein interactions) are relevant for pain after surgery in humans and mice.

Methods: Standardised surgical incisions were performed in male human volunteers and male mice. Quantitative and qualitative sensory phenotyping were combined with unbiased quantitative mass spectrometry-based proteomics and protein network theory. The primary outcomes were skin protein signature changes in humans and phenotype-specific protein-protein interaction analysis 24 h after incision. Secondary outcomes were interspecies comparison of protein regulation as well as protein-protein interactions after incision and validation of selected proteins in human skin by immunofluorescence.

Results: Skin biopsies in 21 human volunteers revealed 119/1569 regulated proteins 24 h after incision. Protein-protein interaction analysis delineated remarkable differences between subjects with small (low responders, n=12) and large incision-related hyperalgesic areas (high responders, n=7), a phenotype most predictive of developing chronic post-surgical pain. Whereas low responders predominantly showed an anti-inflammatory protein signature, high responders exhibited signatures associated with a distinct proteolytic environment and persistent inflammation. Compared to humans, skin biopsies in mice habored even more regulated proteins (435/1871) 24 h after incision with limited overlap between species as assessed by proteome dynamics and PPI. Immunohistochemistry confirmed the expression of high priority candidates in human skin biopsies.

Conclusions: Proteome profiling of human skin after incision revealed protein-protein interactions correlated with pain and hyperalgesia, which may be of potential significance for preventing chronic post-surgical pain. Importantly, protein-protein interactions were differentially modulated in mice compared to humans opening new avenues for successful translational research.

Keywords: acute pain; chronic pain; chronic post-surgical pain; incision; phenotype; protein-protein interaction; proteomics; surgical pain; translational

Received: 24 May 2022; **Accepted:** 24 October 2022

Editor's key points

- The treatment and prevention of acute and chronic post-surgical pain are often inadequate, and the development of mechanism-based novel analgesics is crucially needed.
- For this purpose, rodent models and human surrogate models of skin incision are highly relevant.
- In this translational research study based on sensory phenotyping combined with quantitative proteomics in male rodent and human models of skin incision, the authors identified specific skin protein signatures that correlated to pain phenotypes.
- These results contribute to identifying candidate proteins to target in therapies to prevent pain chronification after surgery.

Worldwide, more than 300 million people undergo surgery each year. Most of them experience acute pain, and treatment remains inadequate in a very high number of patients.[1] Severe post-surgical pain leads to significant suffering of patients; it hampers recovery by impairing mobilisation and physiotherapy and delays discharge.[2] Even more challenging are long-term consequences, including complications, opioid intake, and chronic post-surgical pain (CPSP),[1–7] affecting patients' quality of life and putting a tremendous burden on patients and the community. Recently, the World Health Organization (WHO) (together with the International Association for the Study of Pain, IASP) released their new International Classification of Diseases 11th Revision (ICD-11) classification codes; this now contains codes for several primary and secondary pain diseases, including CPSP and posttraumatic pain. In fact, they classified CPSP as being of high relevance and the prime candidate for preventive measurements.[7]

Currently, the treatment of acute pain and the prevention of CPSP is inadequate. For acute post-surgical pain, opioids and regional anaesthesia techniques are the most effective. However, both are limited by side-effects, including long-term opioid intake.[4,8,9] Also, thus far, CPSP cannot be prevented by pharmaceutical strategies.[10] Consequently, there is an urgent need for novel, effective, and safe analgesics to treat acute pain and prevent CPSP.

A prerequisite for the development of new treatment options is the discovery of mechanisms underlying different pain aetiologies, such as post-surgical pain. Therefore, rodent models of post-surgical pain have been developed and are increasingly used.[11] These surgical incision models are highly relevant as they provide tremendous insights into the unique pathophysiology of post-surgical pain.[12] However, inherent problems in rodent preclinical pain studies are species-specific differences limiting the translational potential.[13] Human surrogate models could offer a missing link that mimics tissue injury and aspects of pathological pain usually seen in patients.[14] In fact, a human model of skin incision has been established that shows signs and symptoms similar to those of surgical patients, including acute pain and hyperalgesia surrounding the injured tissue.[15] The latter has been shown to serve as a clinically relevant pain phenotype associated with the development of CPSP after different types of surgical procedures.[16,17] However, neither the pathophysiology underlying mechanical hyperalgesia early after surgical incision nor the mechanisms leading to differential development of hyperalgesia across patients (i.e. mechanisms that may serve as risk factors for CPSP), have been investigated thus far.

Here, we hypothesised that sensory phenotyping combined with quantitative proteomics could reveal unprecedented insights into species-specific and phenotype-related peripheral processes relevant to acute pain, hyperalgesia, and CPSP development. This study aims at identifying regulated proteins, phenotype-specific skin protein signatures for post-surgical pain, and interspecies similarities and differences to optimise translational research in this field.

Methods

A detailed description of the methodology is provided in Supplementary Material.

Ethics approval/registration

All human experiments were approved by the local Ethics Committee of the Medical Faculty Muenster (registration number 2018-081-b-S), registered in German Clinical Trials Registry (DRKS-ID: DRKS00016641), and in accordance with the latest version of the Declaration of Helsinki. The animal experiments were reviewed and approved in accordance with the recommendations of the ARRIVE guidelines 2.0.[18]

Human volunteers

Enrolled male volunteers (n=26, Fig 1) passed our inclusion criteria (Supplementary Material), were informed about the procedure before the study and provided written informed consent. All volunteers completed a set of psychological questionnaires and a self-rating instrument for assessing pain sensitivity[19–22] (Supplementary Material).

Quantitative sensory testing in human volunteers

Before incision, a comprehensive battery of quantitative sensory testing (QST) was applied to each volar forearm aspect to assess the perception of non-painful and painful stimuli of different modalities (thermal, mechanical, pressure, vibration) established by the German Research Network in Neuropathic Pain.[23] QST parameters were measured in their physical dimension and were weighted by transformation to the standard normal distribution (Z-transformation). Z-scores indicate a gain (above '0') or a loss (below '0') of function.

Incision injury model in human volunteers

The experimental incision proceeded in the volar forearm as previously described.[15] Test and control sides were randomised beforehand. Briefly, for skin incision, the skin was disinfected (ethanol 70%) and incised 4 mm wide and 7 mm deep, perforating the skin and muscular fascia using a scalpel.

Ongoing pain in humans

Using the numeric rating scale (0–100), the volunteers were asked to rate the intensity of ongoing pain before the incision

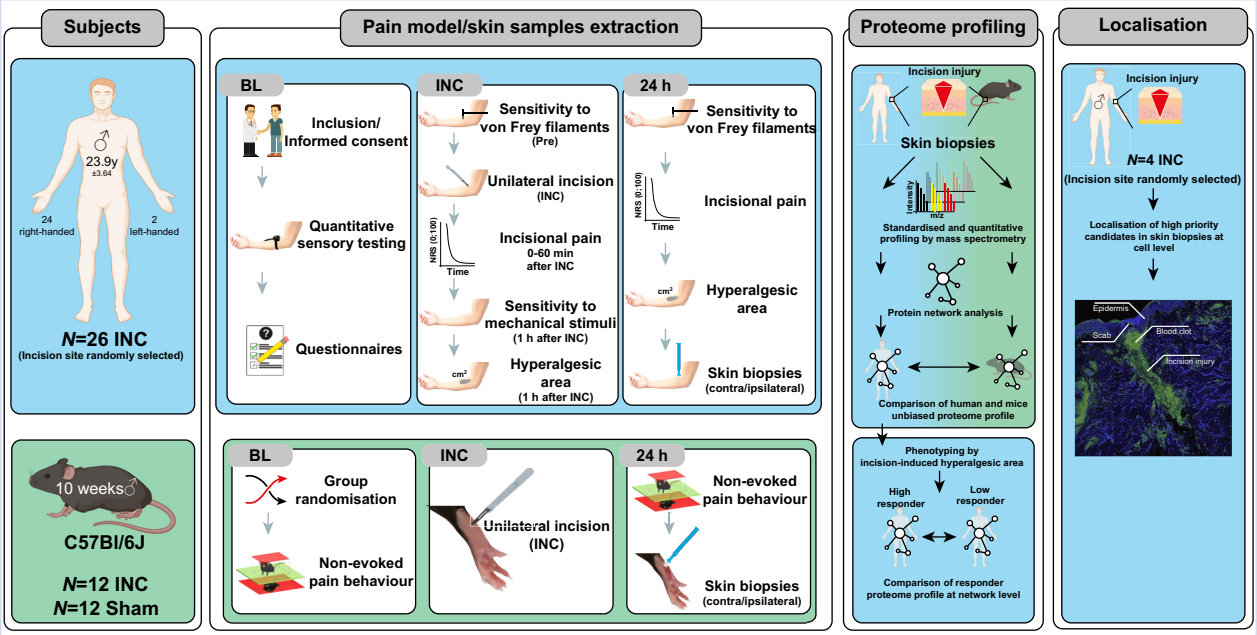

Fig 1. Study design. The study contains four major parts: (1) psycho-physics characterisation of human volunteers (blue) and behaviour tests in mice (green), (2) experimental pain model induction and skin sampling, (3) proteome profiling of incised skin from humans and mice, and (4) immunohistochemistry of high priority candidates in human skin post incision. In total, 30 human male volunteers (26 right-handed) with a mean age of 23.9 yr were included. Mouse experiments were performed with 12 incision- (INC) and 12 sham-treated C57Bl/6J male mice (10 weeks old). Experiments were performed at three different time points: 1 day before incision (baseline, BL), at incision (INC) day, and 24 h after incision. Skin biopsies (ipsilateral and contralateral), including epidermis and fascia, were analysed by quantitative mass spectrometry. Protein-protein interaction network analysis was performed across both species and phenotypic groups (i.e. high or low responder types) in humans. Expression of priority candidates was investigated in skin samples 24 h after incision.

(baseline), during, and after incision for 1 h (first, every minute for 10 min, then every 5 min) and at 4 h and 24 h after the incision.

Mechanical hyperalgesia and mechanical hyperalgesic area

For mechanical pinprick hyperalgesia around the incision, mechanical pain sensitivity and pain thresholds were assessed with a radius of 5 mm around the incision (primary hyperalgesia) and 15 mm around the incision (secondary hyperalgesia). Furthermore, the area of punctate hyperalgesia was determined using an octagram, the vertices of which were determined by a usually non-painful punctate mechanical stimulus (von Frey filaments, 116 mN). The octagon's area represents the area of punctate mechanical hyperalgesia. Testing was performed in random order at the incision and the contralateral site before incision, 1 h, and 24 h after incision.

Plantar incision in mice

Adult male C57Bl/6J mice (n=24 mice, 10 weeks, weight 25.4 [standard deviation 1.8] g were kept in a 12/12 h day/night cycle under standardised specific pathogen-free conditions. An incision was performed in 12 mice under general isoflurane anaesthesia under sterile conditions on the plantar aspect of the right hindpaw.[24] The skin incision was closed with one mattress suture of 6–0 prolene. Sham (control) mice (n=12) were anaesthetised for the same duration, but no incisions and sutures were performed.

Non-evoked pain behaviour in mice

The unbalanced weight-bearing caused by guarding the incised hindpaw was used to assess non-evoked pain behaviour.[25] Briefly, the green illuminated hindpaw area was determined, and the ratio between the contralateral (control) and the incised site was calculated from 10 images over 10 min. All mice were included for proteomic analysis.

Biopsies and sample preparation

The incised skin (or control skin) was removed by 4 mm skin punch biopsies. In humans, both incision (ipsilateral) and contralateral skin samples were obtained after local anaesthesia 24 h after incision. One skin biopsy was performed on each mouse after euthanisia with CO_2. The biopsies contained epidermis and dermis compartments.

Biopsies were homogenised and solubilised as described.[26] Samples from three mice were pooled to obtain four biological replicates. Human biopsies were treated individually. Protein concentrations were determined, and the digestion protocol was based on the paramagnetic bead-based approach. Three volunteers were excluded as a result of the high lipid content in the sample.

Mass spectrometry

Peptides were separated and directly injected into a Q-Exactive HF-X Orbitrap mass spectrometer (Thermo Fisher Scientific, Waltham, MA, USA). Raw data were acquired in data-

independent acquisition (DIA) mode. A detailed description of the methodology is provided in Supplementary Material. Poor mass spectrometry (MS) chromatograms caused the exclusion of two human biological replicates and two pooled mice samples.

DIA-MS data analysis

The DIA raw files were analysed, and spectra were searched against human or mouse Uniprot FASTA databases. A strict quantification filter was applied to assess differential protein abundances between samples. A detailed description of the methodology is provided in Supplementary Material. Mean $\log_2$ ratios were calculated, and pairwise *t*-tests were performed. Obtained *P*-values were adjusted using the Benjamini–Hochberg procedure for multiple testing. Significantly regulated proteins were defined as having a Benjamini–Hochberg-adjusted *q*-value of <0.05. All data have been deposited to the ProteomeXchange Consortium[27] with the dataset identifier PXD030828.

DIA-MS dataset after analysis

For all proteome comparisons, we used the following cut-off: proteins that exhibited $q<0.05$ and $|\log_2 FC| > 0.38$ when comparing human biopsy B_{ipsi} with B_{con} or B_{inc}Mouse (M) with B_{sham}M. Proteome comparisons were made with respective gene names. If two or more gene names are reported for a single protein, we used the first gene name.

Comparisons:

(i) Human B_{inc} *vs* B_{con} for responder types within the hyperalgesic area, 24 h after incision, and time course. Proteins that were exclusively regulated in only one responder type were defined as being up- or downregulated in one responder type and not being regulated at all ($q>0.05$) in the other responder type.
(ii) Human B_{inc} *vs* B_{con} across all volunteers compared with mouse B_{inc}M *vs* B_{sham}M.

Immunohistochemistry staining in human skin

In incisional wounds, immunohistochemical staining visualized matrix metalloproteinases 9 (MMP9) and neutrophil elastase (ELANE). Z-stacks were combined to produce a maximum z-projection. The intensity settings of individual channels were adjusted to meet the average minimum/maximum value across all biological replicates within each technical procedure.

Primary and secondary outcomes

The primary outcome was to identify a cutaneous proteome signature, associated functional pathways, and protein-protein interaction (PPI) networks after incision injury in human volunteers and their specific pain phenotypes (e.g. the area of mechanical hyperalgesia). We identified functional protein pathways using gene ontology (GO) pathway and Reactome analysis via the web-based interface STRING (https://string-db.org/).

Term-term interaction, PPI networks, and network topology analysis were performed by ClueGO (v2.5.8, cytoscape.org[28]) as functional clusters (AutoAnnonate 1.3, cytoscape.org[28]). StringAPP in Cytoscape (3.8.2, cytoscape.org[28]) was used to identify species and pain phenotype-specific protein networks. Functional grouping was performed with AutoAnnonate 1.3. Significantly (*P*-values ≤ 0.05) enriched GO terms were seen in a functionally grouped network that reflects the terms' relationships.

The secondary outcomes were the interspecies comparison of protein regulation and PPI after incision and immunofluorescence validation of selected proteins in human skin. For species comparison, we first identified functional protein pathways in mice after incision and performed the outlined analysis. Then, we compared mice data with human data. For immunofluorescence validation, the cellular localisation of proteins that play a central role in incision-induced networks in humans was analysed by immunohistochemistry of human skin sections.

Statistical analyses

Corresponding statistical tests are indicated in the respective figure legends and are two-sided. For proteome data analysis, we used the Benjamini–Hochberg-adjusted *P*-value (i.e. *q*-value <0.05) (please see Methods and Supplementary Material for details). All data are represented as mean (standard deviation) unless indicated otherwise.

Sample size estimation

Sample sizes were not determined *a priori*; however, they are in line with standards in the field. All replicates were biological.

Results

Volunteer characteristics

Baseline characterisation was performed to ensure that inclusion criteria were fulfilled and that previous psychiatric diseases or limitations of sensory perception were absent (schematically outlined in Fig 1, Supplementary Material); no volunteer needed to be excluded based on these criteria.

Skin protein signature in humans after incision injury

Proteomic analysis of 21/26 human skin biopsies (B) from 'within' the incision (B_{inc}) and in the corresponding area of the contralateral site (B_{con}) resulted in a highly reproducible list of 1569 proteins 24 h after incision (Supplementary Material). Unsupervised hierarchical clustering and principal component analysis (PCA) showed the expected proteome signature segregation (Fig 2a and b). Specifically, 119/1569 quantified proteins were significantly and robustly regulated after incision (Fig. 2c); 73 proteins were up- and 46 downregulated and predicted to be localised in diverse cellular components (Supplementary Material).

Regulated proteins were associated with distinct GO terms for molecular function (MF) and immune system processes (ISP) (Fig 2d). Accordingly, hub-related GO enrichment analysis (Fig 2e and f) highlighted eight major clusters. Among them, the cluster *immune response regulation* was most prominent and included the GO_MF terms *regulation of lymphocyte proliferation*, *oxidoreductase*, and *antimicrobial humoral response* (Fig. 2d–f).

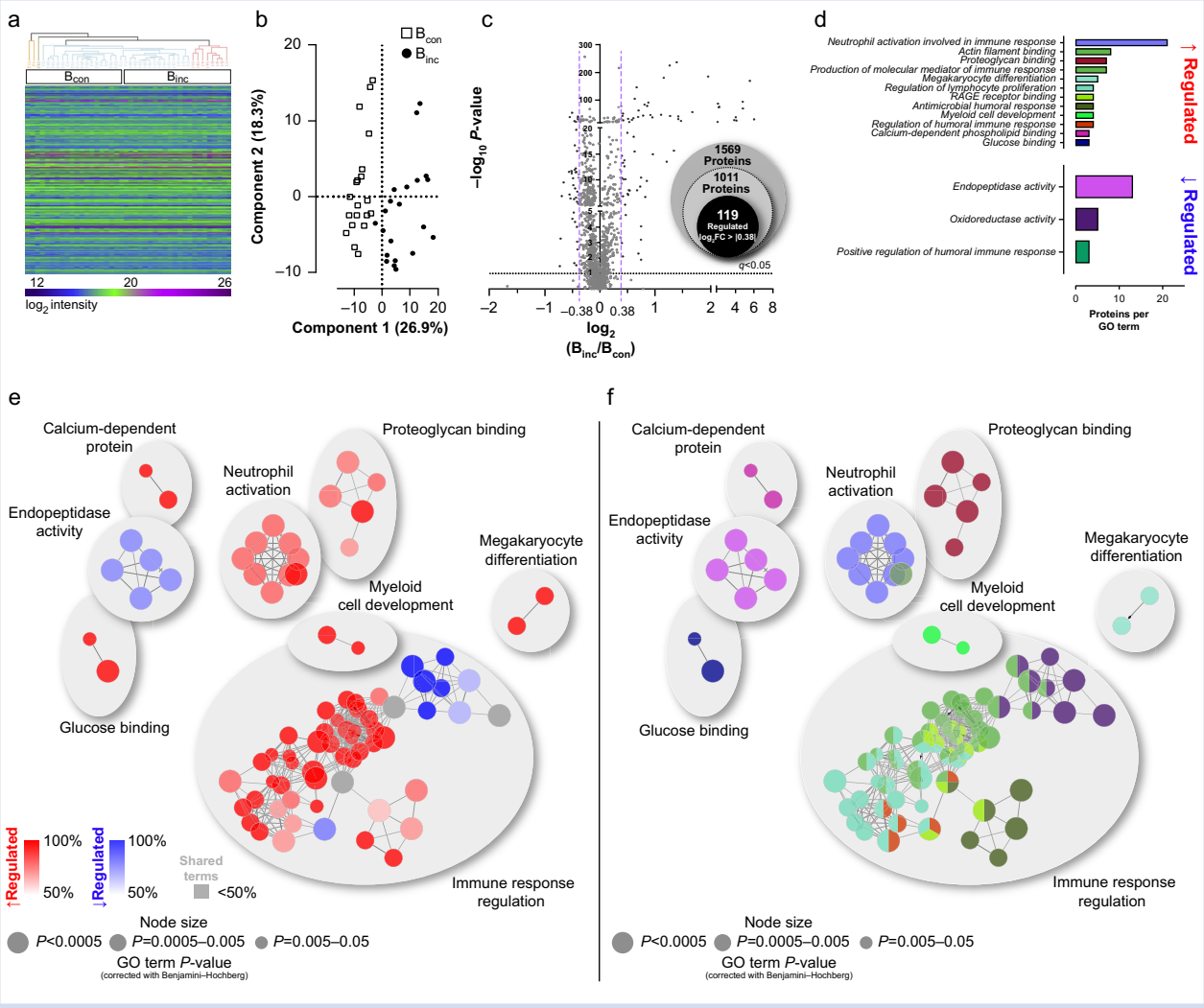

Fig 2. Unbiased protein profiling in human skin upon incision injury. (a) Unsupervised hierarchical clustering of log_2 protein intensities measured by data-independent acquisition-mass spectrometry (DIA-MS) across all skin biopsies (n=21) (contralateral [B_{con}] and incision [B_{inc}]). The legend colour bar indicates the range of log_2 intensity within rows. (b) Principal component analysis separated the proteome signatures of skin biopsies (B) with incision (B_{inc}) compared with the contralateral site (B_{con}) with component 1 by 26.9% and component 2 by 18.3%. (c) In total, 1569 proteins (grey-coloured) were quantified, among which the abundance of 119 proteins (~7.6% of all quantified proteins, black-coloured) were altered upon incision. Proteins were considered as being significantly regulated if they exhibited q<0.05 (q-value represents the corrected P-value; horizontal dotted line) with $log_2FC>|0.38|$ (pink vertical dotted line). (d) Gene ontology (GO) pathway (GO_molecular function and GO_Immun system process) analysis of regulated (upregulated in red; downregulated in blue) proteins in ClueGO (v2.5.8). Only pathways with $P \leq 0.05$ (Benjamini–Hochberg corrected) are shown. (e) (f) Enriched term-term interaction (TTI) network analysis of regulated proteins functionally grouped by ClueGO (v2.5.8) in clusters (AutoAnnonate 1.3). Each node represents a molecular function or immune system process. Node colours are associated with (e) protein regulation (upregulated in red; downregulated in blue) and (f) function (description of the terms, please see (d)). Grey nodes harbour proteins from both regulatory lists and cannot be unambiguously assigned. TTI represents edges between nodes and dots. The size of nodes reflects the significant enrichment of the terms as indicated in the legend.

Pain-related phenotyping reveals human responder types with distinct protein-protein interaction signatures

We aimed to determine whether incision-related phenotypes at given time points after incision could be correlated with obtained snapshots of incision-induced protein signature alterations (Fig 2). We categorised volunteers according to the size of the hyperalgesic area, both 1 h and 24 h after incision (hyperalgesic area time course, HATC, Fig 3a), and, separately, 24 h after incision (HA24) (Supplementary Material). High and low responder categorisation was based on pain phenotype data from this volunteer population; we used the mean and 95% confidence interval as the cut-off. Consequently, volunteers above and below the 95% confidence interval were categorised as high responders and low responders, respectively. We then performed phenotype-dependent proteomic data analysis to identify distinct protein regulations in each responder type. Responder type comparison revealed overlapping proteins (e.g. 51 for HATC, Figs 3b and 54 for HA24,

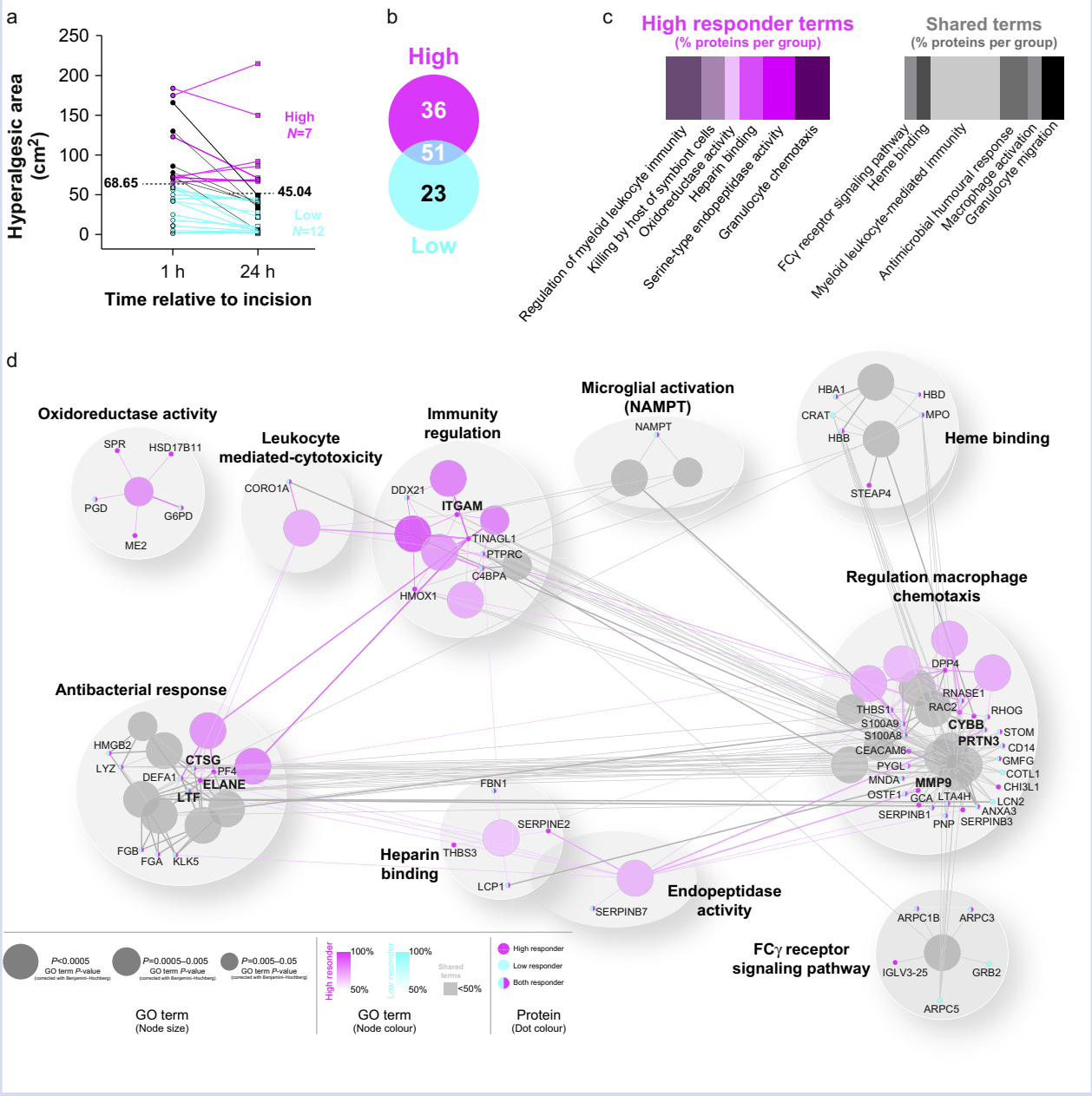

Fig 3. Dominance of high responder term-term interaction networks after incision. (a) After a skin incision, a hyperalgesic area developed around the wound over time, as expected. Human volunteers were phenotyped according to the dimension of hyperalgesic area (cm^2) at 1 and 24 h after incision (HATC; individual values are connected by a line), and, accordingly, categorised into high (n=7, magenta), low (n=12, cyan), and undefined (n=7, black) responders. HATC categorisation was performed by using the mean value (HA1, mean 68.65, HA24, mean 45.04 cm^2, black dotted lines). (b) Distinct and overlapping protein regulations in each responder type. Numbers indicate the number of significantly regulated proteins (q<0.05; $\log_2$FC>|0.38|). (c) Gene ontology (GO) analysis revealed annotations of regulated proteins, specifically in high responders (magenta shades). Shared terms belong to both responder types (grey shades). In contrast, regulated proteins identified in low responders could not be annotated to distinct pathways. (d) Enriched term-term interaction (TTI) network analysis with associated proteins was functionally grouped by ClueGO (v2.5.8) as functional clusters (AutoAnnonate 1.3). Data information: significantly (P-values ≤0.05, Benjamini–Hochberg corrected) enriched GO terms seen in a functionally grouped network that reflects the terms' relationships. Each node represents a molecular function or immune system process; node colours are associated with phenotyping (high responder in magenta shades; low responder in cyan shades). Grey shades reflect unspecific terms which belong to both responder types. Proteins are displayed as dots in responder-type colours (magenta=high responder, cyan=low responder, colour shared=responder independent). The degree of connectivity between terms (kappa score=0.3) was used to define functional groups. TTI represents edges between nodes and dots. The size of nodes reflects the significant enrichment of each term. ELANE, neutrophil elastase; MMP9, matrix metalloproteinase 9.

Supplementary Material) and, interestingly, proteins uniquely regulated either in high or low responders. Focusing on HATC data (Fig 3), GO analysis identified terms only present in high responders, such as *oxidoreductase* and *serine-type endopeptidase activity* (Fig 3d) and predicted 10 biological clusters with their associated proteins (Fig 3d). Cluster-associated proteins regulated in high responders, such as ELANE, MMP9, CYBB, and ITGAM, exhibited high cluster-cluster or cluster-protein interactions.

Responder-type PPI architecture was then analysed by topology features and protein attributes (Fig 4 and Supplementary Material). High responder networks contained seven highly connected (degree >8) nodes compared with only one such node in low responder networks (Fig 4a). The higher degree of connectivity was accompanied by high network density, edge number and, in some cases, high betweenness centrality, especially for the two hub proteins (i.e. MMP9 and ITGAM) (Fig 4b).

Based on our data (Fig 4), MMP9 and ELANE appear to play a central role in high responders after incision. Immunostaining revealed that MMP9 and ELANE were colocalised with CD66b+ cells (neutrophil granulocytes) within the incision in human skin (Fig 4c and d). In addition, MMP9+ cells were present in the epidermis (likely keratinocytes) and the dermis (likely endothelial cells and mast cells) on ipsi- and contralateral sides. ELANE was colocalised with neutrophil granulocytes within the incision but absent in the epidermal layer (Supplementary Material).

Skin protein signature in mice after incision and comparison with humans

Unsupervised hierarchical clustering and PCA (Fig 5a and b) revealed proteomic signatures of 1871 proteins in mice 24 h after incision. A total of 435/1897 proteins had significant and robust abundance changes compared with sham, with 175 being upregulated and 260 being downregulated (Fig 5c, Supplementary Material). Functionally distinct GO_MF and GO_ISP were observed among regulated proteins (Fig 5d). Hub-related GO enrichment analysis revealed 22 clusters, among which *complement activation* was highly prominent and contained mainly upregulated hubs (Fig 5e and f). Next, we aimed to assess interspecies similarities and differences in protein signatures and their incision-induced dynamics (Fig 6). In total, the overlap between species encompasses 1159 proteins. However, 712/1897 mouse proteins were not reliably detected in all humans and vice versa for 410/1569 human proteins (Fig 6a). However, this does not mean that respective proteins are missing in a species. Instead, they might not have reached our highly stringent detection and quantification criteria (Supplementary Material for details). After incision, 50 regulated proteins were shared among species (Fig 6a and b). Notably, the direction of the regulation was highly conserved (Fig 6b) with few exceptions (Fig 6c). Human skin exhibited noticeable changes in proteins annotated to *extracellular matrix organisation*, a relatively underrepresented pathway in mice (Fig 6d). In contrast, *post-translational protein modification* and *metabolism of proteins* were significantly more enriched in mice. In terms of PPI networks, *platelet aggregation*, *inflammatory activity*, and *actin polymerisation* represented prominently altered clusters in both species (Fig 6e). Annotated upregulated proteins, such as FN1, FERMT3, and LCP1, exhibited a high connectivity degree and betweenness centrality (Fig 6e).

Discussion

An unbiased quantitative proteomics approach was applied to elucidate (i) incision-induced PPI networks in humans, (ii) phenotype-specific PPI networks, and (iii) conserved interspecies (human *vs* mouse) overlaps. Pain phenotyping paired with quantitative proteomics deciphered unique insights into cutaneous PPI modulated within 24 h of an incision. These may mechanistically govern incision-related symptoms, such as mechanical hyperalgesia, known to be relevant for chronification of post-surgical pain in patients.

Previously, single candidate molecules associated with incision-induced nociceptor activation and sensitisation causing pain and hyperalgesia have been identified predominantly using rodent incision models.[11,12,29] Yet the complexity of incision-induced proteome dynamics underlying hyperalgesia is unknown, and translation from animals to humans is challenged by interspecies differences in skin layer thickness, immune cells, and wound healing strategies (see limitations below). However, despite these differences and the fact that different skin types (i.e. hairy skin [human] *vs* glabrous skin [mice]) are injured, it is all the more remarkable that we found interspecies similarities in inflammatory activity on network and protein levels (e.g. FERMT3, FN1, and LCP1) in line with sensory phenomena such as mechanical hypersensitivity upon incision.[11,15] These similarities may indicate an evolutionarily conserved interplay between inflammatory mediators and activation/sensitisation of nociceptive terminals, which requires further exploration. However, our present data also highlight substantial species differences after incision and may explain the low success of translating findings from rodents to humans. Only a few reports compared rodent and human tissue in a parallel and unbiased manner in the context of pain.[30,31] Previous transcriptomic studies of peripheral nerves[30] and dorsal root ganglia[31] indicated interspecies similarities and differences. However, none of these reports assessed proteome signatures, and we still lack insights into incision-induced plasticity at the protein and, importantly, the PPI network level. Our study fills this gap. Overall, the presented incision-induced PPI signatures highlight both interspecies similarities and differences—a prerequisite for successful forward and reverse translational research.

Sensory profiling data were harnessed to stratify volunteers, thus strongly suggesting the functional relevance of a suite of proteins and PPI networks. Post-incisional mechanical hyperalgesia is critical because it is correlated with chronification of post-surgical pain.[32,33] In addition, it is a general phenomenon inherent to many human pain models and pain patients, but clinically relevant biomarkers are still lacking.[14] Our results provide unprecedented mechanistic insights into incision injury and, importantly, serve as a stepping stone for phenotype-specific sub-grouping of pain-related symptoms via protein signatures. In particular, we predict a proteolytic environment with a hypercatabolic state, resulting in a prolonged immune response in patients developing more hyperalgesia than others (high responder). Proteases (e.g. MMP9 and ELANE) in central network positions represent the proteolytic environment, potentially causing an extracellular matrix deposition and degradation imbalance. This may trigger increased immune cell migration and overactivation of the inflammatory response, which may prolong sensitisation of peripheral nociceptors, resulting in a hyperalgesic phenotype in high responders. In turn, the nociceptor sensitisation may

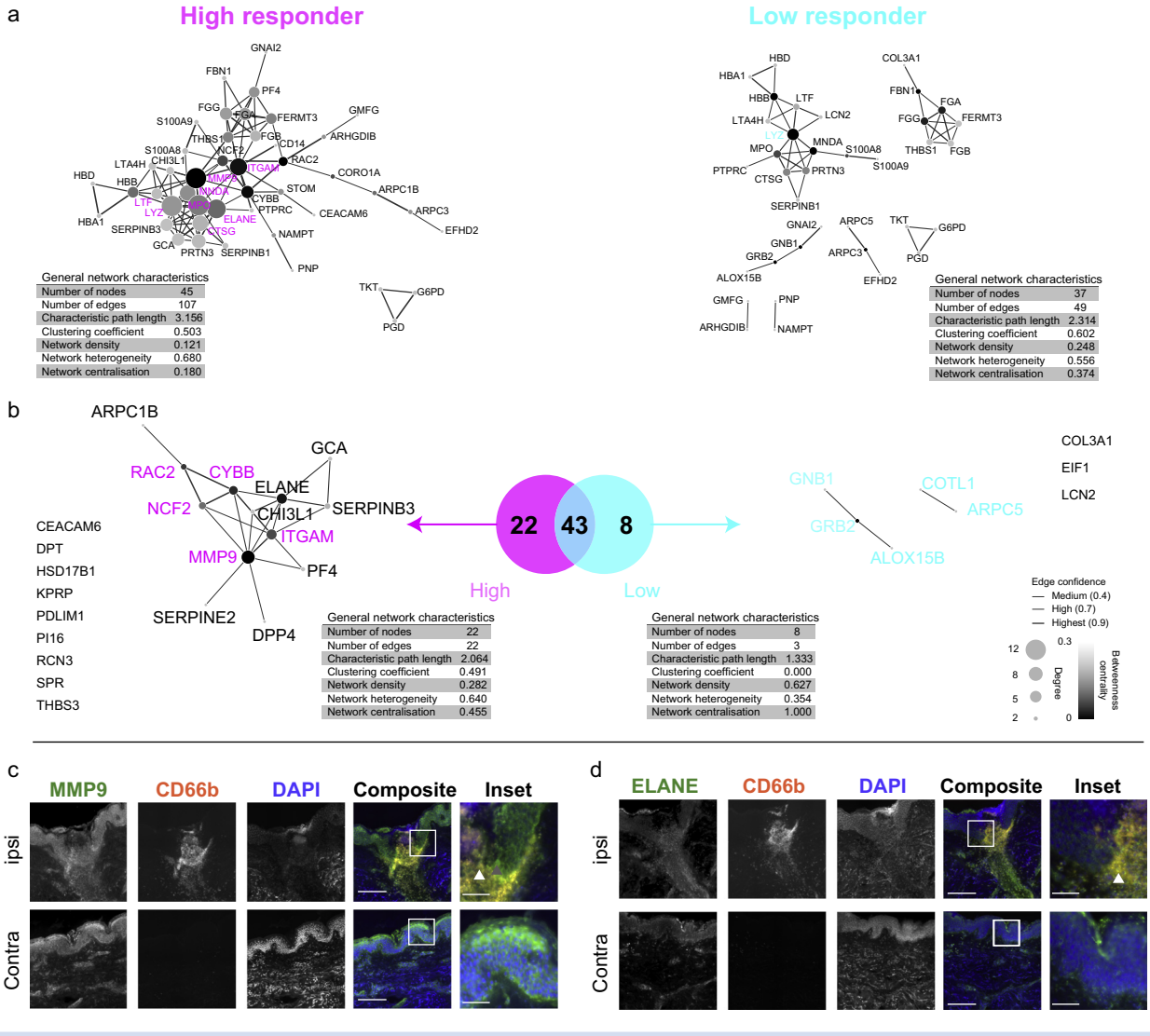

Fig 4. Skin incision induces a distinct protein-protein interactions network topology in dependence on responder types. (a) Enriched protein-protein interaction (PPI) network for responder types after incision (magenta, high responder; cyan, low responder) derived from merged networks (Supplementary Fig. S5). (b) Differential PPI networks when comparing high (magenta) and low (cyan) responder types. Unique PPI networks are displayed. Unlinked proteins are shown as names only, without a sphere. (c) Upon incision, MMP9 colocalised with CD66b+ cells (neutrophils, see inset, white arrow) within the incision injury and in the epidermis (see inset, dark grey arrow) of the ipsilateral side. Marginal MMP9 and CD66b signals were detected on the contralateral side with the exception of the epidermis. (d) Upon incision, ELANE colocalised with CD66b+ cells (neutrophils, see inset, white arrow) within the incision injury (in the epidermis and dermis) on the ipsilateral side. Additionally, in the dermis, other cell types are ELANE+. Marginal ELANE and CD66b signals were detected on the contralateral side except for the stratum corneum of the epidermis. Data information: enriched (False Discovery Rate, FDR<0.05; assessed via the web-based interface STRING) PPI network topologies of incision-induced phenotypes were analysed by stringAPP in Cytoscape (3.8.2). Nodes represent a single protein, including degree (size) and betweenness centrality (colour). PPI isf (v reflected by edges (thickness represents confidence). Data information: In (a,b), scale bar =500 μm (composite), 200 μm (composite), 50 μm (inset). DAPI, 4′,6-diamidino-2-phenylindole; ELANE, neutrophil elastase; MMP9, matrix metalloproteinase 9.

facilitate central sensitisation processes causing large hyperalgesic areas and chronification processes, including CPSP.[34] Our study shows a similar disbalance in proteases and resident immune activation as observed in chronic, unhealed, and painful wounds.[35] In low responders, an opposing picture was evident. Here, anti-inflammatory processes predominated, likely indicating a decrease in inflammation and transition to the remodelling phase.

Our phenotype-specific analysis revealed potential PPI networks that might be suitable targets for future therapeutic and diagnostic interventions, such as the prevention of CPSP. Of note, modulation of *central* hub proteins (such as MMP9) within such a protein network that affects essential physiological aspects (e.g. wound healing) may not be suitable because this could compromise the integrity of the whole network.[36] In contrast, more peripheral network members

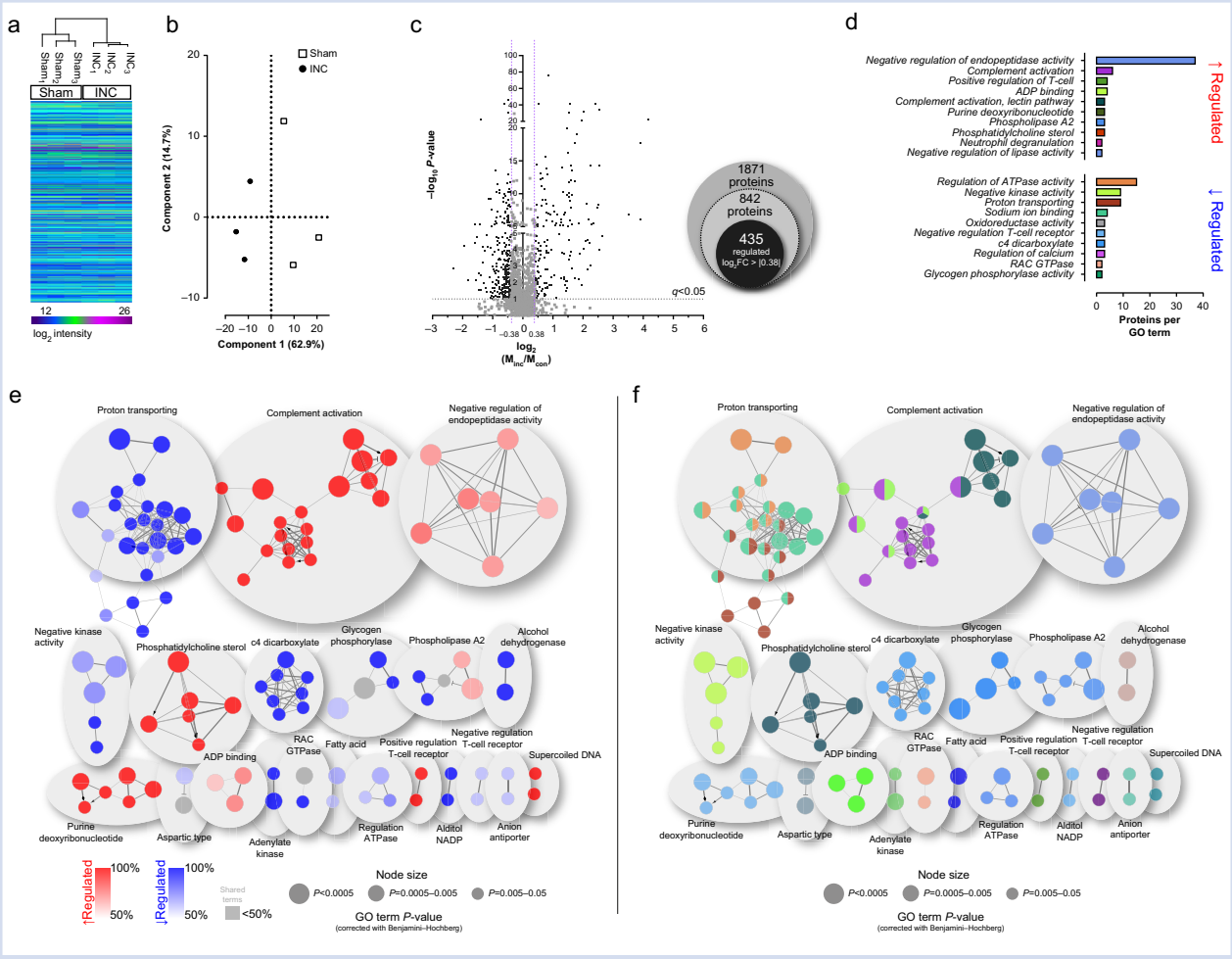

Fig 5. Unbiased protein profiling in mice skin upon incision injury. (a) Unsupervised hierarchical clustering of log_2 protein intensities obtained by quantitative data-independent acquisition-mass spectrometry (DIA-MS) of paw skin biopsies (B) from mice (n=3 biological replicates per condition, N [number of mice]=9 sham, N=9 incision, INC). The legend colour bar indicates the range of log_2 intensity within rows. (b) Principal component analysis separated the proteome signatures of skin biopsies (B) with incision (B_{inc}) compared with the contralateral site (B_{con}) with component 1 by 62.9% and component 2 by 14.7%. (c) In total, 1871 proteins (grey-coloured) were quantified, among which the abundance of 435 proteins (~23.3% of all quantified proteins, black-coloured) were altered upon incision. Proteins were considered as significantly regulated if they exhibited q<0.05 (q-value represents the corrected P-value; horizontal dotted line) with log_2 FC >|0.38| (pink vertical dotted line). (d) Gene ontology (GO) pathway (GO_molecular function and GO_Immun system process) analysis of regulated (upregulated in red; downregulated in blue) proteins in ClueGO (v2.5.8). Only pathways with $P \leq 0.05$ (Benjamini–Hochberg corrected) are shown. (e) (f) Enriched term-term interaction (TTI) network analysis of regulated proteins functionally grouped by ClueGO (v2.5.8) in clusters (AutoAnnonate 1.3). Significantly (p-values ≤0.05, Benjamini–Hochberg corrected) enriched GO terms are seen in a functionally grouped network that reflects the terms' relationships. Each node represents a molecular function or immune system process. (e) Node colours are associated with protein regulation (upregulated in red; downregulated in blue) and (f) function. The degree of connectivity between terms (kappa score) was used for defining functional groups (highlighted in colour; see in [d]). Grey nodes harbour proteins from both regulatory lists and therefore cannot be unambiguously assigned. TTI is represented by edges between nodes and dots. The size of nodes reflects the significant enrichment of each term, as indicated in the legend.

may represent preferred targets. Topological properties, eccentricity, and modularity should be used to select potential drug target proteins as a proxy for their ability to (i) interfere with network-relevant proteins or (ii) functionally affect related proteins within the network.[37]

Specific aspects and limitations need to be considered when interpreting our results. Given budget constraints, only skin biopsies from male volunteers and male mice were used in this work. This might be a limitation given known sex differences in pain,[13] including incisional pain.[15] Whether there are also gender-specific differences in the skin's proteome after an incision will need to be addressed in future studies. Second, samples were obtained from hairy skin (humans) and glabrous skin (mice) within the incision site and contained proteins of several cell types. The comparison between these different skin types in humans and rodents paired with different wound healing strategies[38] is a limitation of this study and similar studies in the field. Pain models in humans

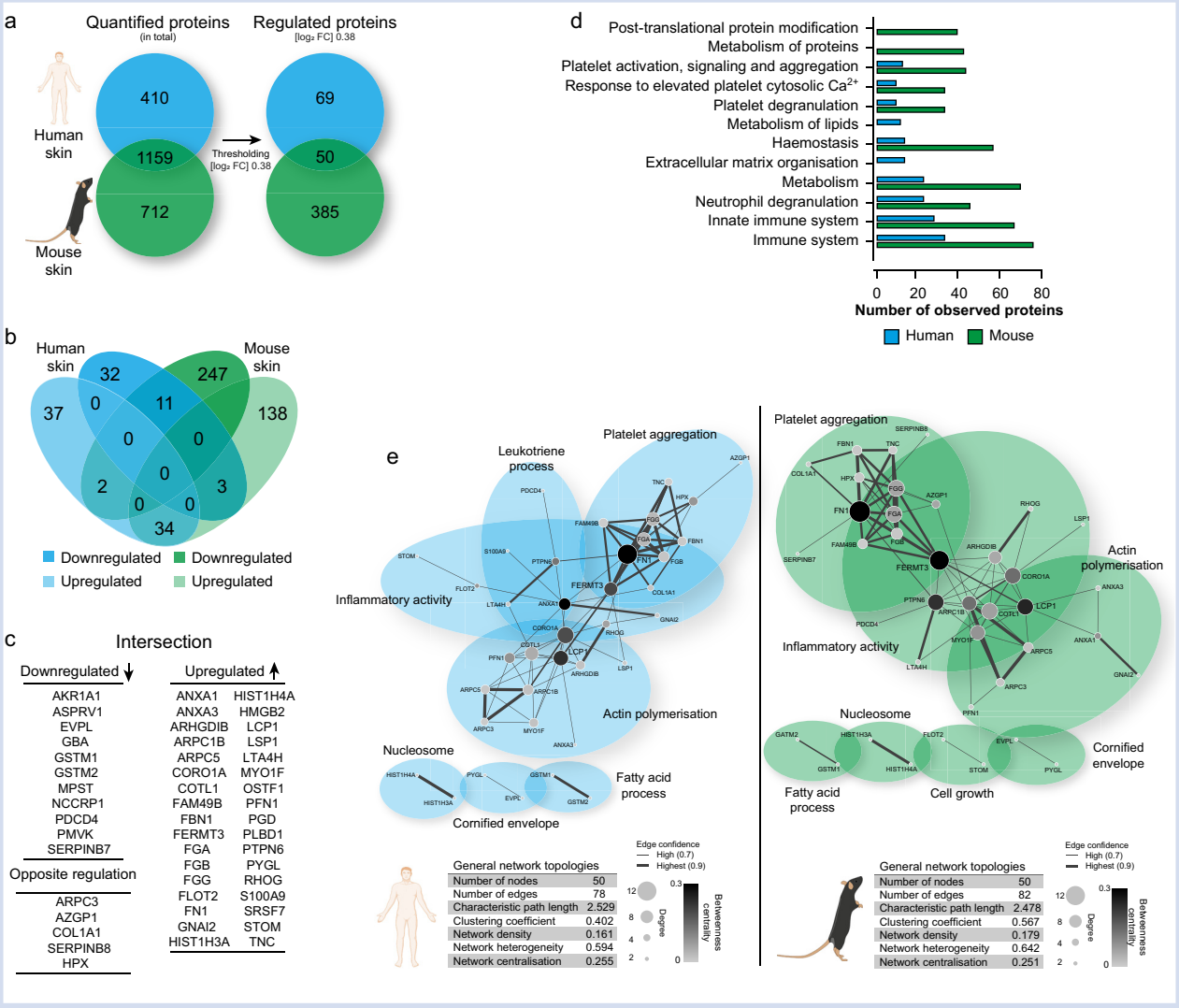

Fig 6. Incisional injury affects distinct cutaneous protein signatures in human and mouse skin biopsies. (a) Comparison of quantified and significantly regulated (q<0.05; log2FC>|0.38|) proteins in human and mouse skin biopsies. (b) Venn diagrams display the comparison of regulated proteins in human and mouse skin biopsies. Proteins regulated in both species (intersections) are listed in (c). (c) List of the 50 shared proteins which appear to be regulated in both species upon incision. (d) Gene ontology (GO) pathway and Reactome analysis in both species (human: blue, mice: green). Only the top 10 pathways, which exhibit significant enrichment (False Discovery Rate, FDR<0.05; assessed via the web-based interface STRING), are displayed. (e) Enriched protein-protein interaction (PPI) network of regulated and shared proteins in humans and mice. (FDR<0.05; assessed via the web-based interface STRING). Data information: network topology was analysed by stringAPP in Cytoscape (3.8.2). Each node represents a single protein, with information on the degree (size) and betweenness centrality (colour). PPI networks are reflected by edges (thickness represents confidence). Functional grouping was performed with AutoAnnonate 1.3.

and mice have been established at these different sites mainly because of practical and ethical issues. Nonetheless, and despite cell-based differences in skin anatomy, incision injury shows a significant interspecies overlap of incision-related phenotypes, such as mechanical hyperalgesia, highlighting the translational potential of our study regardless of skin type. Previous work has extensively characterised mouse skin cell types using transcriptomics.[39] Our work considerably extends these efforts by providing interspecies proteome profiles, altered interspecies protein signatures, and their correlation with pain-associated phenotypes in humans. This is of high significance, as the correspondence of the transcriptome with the proteome is known to be limited, causing significant challenges in predicting functional alterations on the mRNA level.[40]

In summary, we identified, for the first time, human phenotype-specific protein-protein interaction networks upon skin incision, potentially highlighting new targets for acute and chronic post-surgical pain. Our results may provide a stepping stone to identify and modulate (multiple) candidate proteins within PPI networks that could be harnessed to ameliorate post-surgical consequences and, consequently, prevent pain chronification. We uncovered species-specific differences and similarities in incision-induced skin protein signatures, alerting the community to the challenges of bidirectional translational approaches. Finally, we pinpoint

hitherto unknown molecular aspects of back-translation into the mouse, which need to be considered in future investigations.

Authors' contributions

Study design: DS, MS, EPZ
Experiments: DS, MvdB, CK, DSG, JS, SB, BD, MS, EPZ
Data analysis: DS, CK, DSG, JS, BD, DGV, MS
Writing first manuscript draft: DS, MS, EPZ
Figure preparation: DS, MS, EPZ, CK, DGV
Revising manuscript: MvdB, CK, DSG, JS, SB, BD, DGV, PKZ

Declarations of interest

MS received research awards and travel support by the German Pain Society (DGSS) both of which were sponsored by Astellas Pharma GmbH (Germany). MS received one-time consulting honoraria by Grunenthal GmbH (Germany). None of these funding sources influenced the content of this study, and MS declares no conflict of interest. During the past 5 yr, EPZ received financial support from Grunenthal for research activities and from Grunenthal, Novartis (Switzerland), Medtronic for advisory board activities, lecture fees, or both. None of this research support/funds was used for or influenced this manuscript, and EPZ declares no conflict of interest. The remaining authors declare that they have no conflicts of interest.

Funding

Deutsche Forschungsgemeinschaft (DFG) (SCHM 2533/6–1 and SCHM 2533/4–1 to MS, GO2481/3–1 to DGV, PO1319/3–1 to EPZ). Federal Ministry of Education and Research (BMBF), Germany, to EPZ (01KC1903). University of Vienna to MS.

Appendix A. Supplementary data

Supplementary data to this article can be found online at https://doi.org/10.1016/j.bja.2022.10.040.

References

1. Gerbershagen HJ, Aduckathil S, van Wijck JM, et al. Pain intensity on the first day after surgery: a prospective cohort study comparing 179 surgical procedures. *Anesthesiology* 2013; **118**: 934–44
2. van Boekel RLM, Warlé MC, Nielen RGC, et al. Relationship between postoperative pain and overall 30-day complications in a broad surgical population: an observational study. *Ann Surg* 2017; **269**: 856–65
3. Sun EC, Darnall BD, Baker LC, et al. Incidence of and risk factors for chronic opioid use among opioid-naive patients in the postoperative period. *JAMA Intern Med* 2016; **176**: 1286–93
4. Glare P, Aubrey KR, Myles PS. Transition from acute to chronic pain after surgery. *Lancet* 2019; **393**: 1537–46
5. Fletcher D, Stamer UM, Pogatzki-Zahn E, et al. Chronic postsurgical pain in Europe: an observational study. *Eur J Anaesthesiol* 2015; **32**: 725–34
6. Gan TJ, Habib AS, Miller TE, et al. Incidence, patient satisfaction, and perceptions of post-surgical pain: results from a US national survey. *Curr Med Res Opin* 2014; **30**: 149–60
7. Schug SA, Lavand'homme P, Barke A, et al. The IASP classification of chronic pain for ICD-11: chronic postsurgical or posttraumatic pain. *Pain* 2019; **160**: 45–52
8. Macintyre PE, Quinlan J, Levy N, et al. Current issues in the use of opioids for the management of postoperative pain: a review. *JAMA Surg* 2022; **157**: 158–66
9. Weibel S, Jelting Y, Pace NL, et al. Continuous intravenous perioperative lidocaine infusion for postoperative pain and recovery in adults. *Cochrane Database Syst Rev* 2018; **6**: CD009642
10. Carley ME, Chaparro LE, Choinière M, et al. Pharmacotherapy for the prevention of chronic pain after surgery in adults: an updated systematic review and meta-analysis. *Anesthesiology* 2021; **135**: 304–25
11. Pogatzki-Zahn E, Segelcke D, Zahn P. Mechanisms of acute and chronic pain after surgery: update from findings in experimental animal models. *Curr Opin Anaesthesiol* 2018; **31**: 575–85
12. Pogatzki-Zahn EM, Segelcke D, Schug SA. Postoperative pain-from mechanisms to treatment. *Pain Rep* 2017; **2**: e588
13. Mouraux A, Bannister K, Becker S, et al. Challenges and opportunities in translational pain research - an opinion paper of the working group on translational pain research of the European pain federation (EFIC). *Eur J Pain* 2021; **25**: 731–56
14. Quesada C, Kostenko A, Ho I, et al. Human surrogate models of central sensitization: a critical review and practical guide. *Eur J Pain* 2021; **25**: 1389–428
15. Pogatzki-Zahn EM, Drescher C, Englbrecht JS, et al. Progesterone relates to enhanced incisional acute pain and pinprick hyperalgesia in the luteal phase of female volunteers. *Pain* 2019; **160**: 1781–93
16. Martinez V, Ben Ammar S, Judet T, et al. Risk factors predictive of chronic postsurgical neuropathic pain: the value of the iliac crest bone harvest model. *Pain* 2012; **153**: 1478–83
17. Kock M de, Lavand'homme P, Waterloos H. Balanced analgesia' in the perioperative period: is there a place for ketamine? *Pain* 2001; **92**: 373–80
18. Du Percie Sert N, Hurst V, Ahluwalia A, et al. The ARRIVE guidelines 2.0: updated guidelines for reporting animal research. *PLoS Biol* 2020; **18**, e3000410
19. Sullivan MJL, Bishop SR, Pivik J. The pain catastrophizing scale: development and validation. *Psychol Assess* 1995; **7**: 524–32
20. Spielberger CD. *Manual for the state-trait anxiety inventory (STAI)*. Palo Alto, CA: Consulting Psychologist Press; 1983
21. Ruscheweyh R, Verneuer B, Dany K, et al. Validation of the pain sensitivity questionnaire in chronic pain patients. *Pain* 2012; **153**: 1210–8
22. Beck AT, Ward CH, Mendelson M, Mock J, Erbaugh J. An inventory for measuring depression. *Arch Gen Psychiatry* 1961; **4**: 561–71
23. Rolke R, Baron R, Maier C, et al. Quantitative sensory testing in the German Research Network on Neuropathic Pain (DFNS): standardized protocol and reference values. *Pain* 2006; **123**: 231–43
24. Pogatzki EM, Raja SN. A mouse model of incisional pain. *Anesthesiology* 2003; **99**: 1023–7

25. Pogatzki-Zahn EM, Gomez-Varela D, Erdmann G, et al. A proteome signature for acute incisional pain in dorsal root ganglia of mice. *Pain* 2021; **162**: 2070–86
26. Bruderer R, Sondermann J, Tsou C-C, et al. New targeted approaches for the quantification of data-independent acquisition mass spectrometry. *Proteomics* 2017; **17**: 1700021
27. Perez-Riverol Y, Csordas A, Bai J, et al. The PRIDE database and related tools and resources in 2019: improving support for quantification data. *Nucleic Acids Res* 2019; **47**: D442–50
28. Lotia S, Montojo J, Dong Y, et al. Cytoscape app store. *Bioinformatics* 2013; **29**: 1350–1
29. Segelcke D, Pradier B, Pogatzki-Zahn E. Advances in assessment of pain behaviors and mechanisms of postoperative pain models. *Curr Opin Physiol* 2019; **11**: 85–92
30. Ray PR, Khan J, Wangzhou A, et al. Transcriptome analysis of the human tibial nerve identifies sexually dimorphic expression of genes involved in pain, inflammation, and neuro-immunity. *Front Mol Neurosci* 2019; **12**: 37
31. Ray P, Torck A, Quigley L, et al. Comparative transcriptome profiling of the human and mouse dorsal root ganglia: an RNA-seq-based resource for pain and sensory neuroscience research. *Pain* 2018; **159**: 1325–45
32. Eisenach JC. Preventing chronic pain after surgery: who, how, and when? *Reg Anesth Pain Med* 2006; **31**: 1–3
33. Lavand'homme P, De Kock M, Waterloos H. Intraoperative epidural analgesia combined with ketamine provides effective preventive analgesia in patients undergoing major digestive surgery. *Anesthesiology* 2005; **103**: 813–20
34. Treede RD, Magerl W. Multiple mechanisms of secondary hyperalgesia. *Prog Brain Res* 2000; **129**: 331–41
35. Holl J, Kowalewski C, Zimek Z, et al. Chronic diabetic wounds and their treatment with skin substitutes. *Cells* 2021; **10**: 655
36. Gu H-W, Xing F, Jiang M-J, et al. Upregulation of matrix metalloproteinase-9/2 in the wounded tissue, dorsal root ganglia, and spinal cord is involved in the development of postoperative pain. *Brain Res* 2019; **1718**: 64–74
37. Feng Y, Wang Q, Wang T. Drug target protein-protein interaction networks: a systematic perspective. *Biomed Res Int* 2017; **2017**, 1289259
38. Zomer HD, Trentin AG. Skin wound healing in humans and mice: challenges in translational research. *J Dermatol Sci* 2018; **90**: 3–12
39. Joost S, Annusver K, Jacob T, et al. The molecular anatomy of mouse skin during hair growth and rest. *Cell Stem Cell* 2020; **26**: 441–57. e7
40. Wang J, Ma Z, Carr SA, et al. Proteome profiling outperforms transcriptome profiling for coexpression based gene function prediction. *Mol Cell Proteomics* 2017; **16**: 121–34

Handling editor: Nadine Attal